

Cryogelation within Cryogels: Silk Fibroin Scaffolds with Single-, Double- and Triple-Network Structures

Berkant Yetiskin, Caner Akinci, Oguz Okay*

Istanbul Technical University, Department of Chemistry, 34469 Istanbul, Turkey

Table of Contents

Table S1. Formation conditions and swelling properties of silk-fibroin cryogels	2
Table S2. Compressive mechanical properties of silk-fibroin cryogels.	4
Figure S1. Typical ATR-FTIR spectra of fibroin scaffolds.	5
Figure S2. Optical microscopy images of SN and DN cryogels.	6
Figure S3. SEM images of DN-4/14 and TN-4/4/14 fibroin scaffolds.	7

Table S1a. Formation conditions and swelling properties of SN cryogels. C_{SF} = fibroin concentration, W_g = gel fraction, $q_{w,i}$, $q_{v,i}$ = weight and volume swelling ratios, respectively. Standard deviations in W_g , $q_{v,i}$, and $q_{w,i}$ are less than 10%. The average β -sheet content of SN, DN, and TN cryogels is 36 ± 7 %. As explained in the manuscript, aqueous fibroin solutions with C_{SF} between 5 and 61.4 wt% were prepared by dialyzing fibroin solutions against aqueous PEG solutions.

C_{SF} wt%	mmol epoxy / g SF	W_g	$q_{v,i}$	$q_{w,i}$	Conformation %			
					β - sheet	Random coil	α - helix	β - turn
1.0	20	2.1	1.33	35	-	-	-	-
2.0	20	1.45	1.09	27	-	-	-	-
3.0	20	1.15	1.43	20	-	-	-	-
4.2	20	1.20	1.11	17	27	43	29	1
11.6	20	0.94	1.21	7.0	34	42	21	2
12.0	20	0.98	1.48	6.8	41	31	25	2
12.6	20	0.87	1.09	7.8	-	-	-	-
13.5	20	1.08	1.19	6.1	32	45	20	2
16.8	13	0.90	1.25	5.4	41	22	34	3
18.6	10	0.82	1.17	5.5	-	-	-	-
18.8	10	1.09	1.21	5.1	31	45	21	2
20.0	6	1.10	1.27	4.1	48	9	40	3
23.5	7	0.89	1.16	4.5	48	22	32	2
23.7	10	0.89	1.26	3.7	31	40	28	2
27.0	10	0.56	1.23	5.2	25	44	29	1
29.1	3.3	0.98	1.16	3.4	35	17	47	1
34.1	2.4	0.58	1.27	5.1	36	46	17	1
39.0	3.4	0.60	1.25	4.0	-	-	-	-
40.0	4.4	0.51	1.08	4.46	37	44	17	1
45.3	3.9	0.43	1.20	4.75	33	46	19	1
46.2	1.3	0.60	1.14	3.61	48	9	40	2
61.4	1.7	0.45	1.23	3.23	36	47	16	1

Table S1b. Formation conditions and swelling properties of DN and TN cryogels together with the precursor SN-4. x, y, z = fibroin concentration in the 1st, 2nd and 3rd fibroin solutions, respectively.

Code	x wt%	y wt%	z wt%	mmol epoxy·g ⁻¹		
				1 st	2 nd	3 rd
SN-4	4.2	-	-	20		
DN-4/7	4.2	7.2	-	20	20	
DN-4/14	4.2	14.3	-	20	10	
DN-4/21	4.2	20.5	-	20	5	
DN-4/29	4.2	28.6	-	20	1.5	
TN-4/7/20	4.2	7.2	20	20	20	5

Code	C _{SF} wt%	W _g	q _{v,i}	q _{w,i}	Conformation %			
					β-sheet	Random coil	α-helix	b-turn
SN-4	4.2	1.20	1.11	17	27	43	29	1
DN-4/7	13.4	1.50	1.27	6.8	33	42	22	2
DN-4/14	21	0.95	1.2	5.1	29	48	21	2
DN-4/21	28	0.92	1.19	4.5	39	37	21	3
DN-4/29	36	1.11	1.2	3.9	36	35	27	2
TN-4/7/20	45.4	1.0	1.2	4.5	39	31	28	2

Table S2. Compressive mechanical properties of silk-fibroin cryogels. C_{SF} = Fibroin concentration, E = Young's modulus, σ_f = fracture stress, σ_{comp} = stress at 3% compression, $\sigma_{plateau}$ = plateau stress. Numbers in the parentheses are standard deviations.

C_{SF} wt%	E / MPa		σ_f / MPa		σ_{comp} / MPa		$\sigma_{plateau}$ / MPa	
	dry	Swollen	Dry	swollen	dry	swollen	dry	swollen
4.2	7 (2)	0.034 (0.004)	16 (2)	9.3 (0.1)	0.13 (0.02)	0.0080 (0.0001)	0.32 (0.01)	0.0085 (0)
7.5	12 (2)	0.044 (0.015)	31 (1)	9.0 (0.1)	0.24 (0.07)	0.0089 (0.0004)	0.68 (0.01)	0.012 (0.001)
11.6	18 (0)	0.5 (0.1)	40 (20)	18 (3)	0.39 (0.01)	0.021 (0.004)	1.06 (0.22)	0.046 (0.004)
12.6	27 (10)	-	-	-	0.53 (0.14)	-	1.61 (0.12)	-
13.5	37 (9)	-	-	-	0.97 (0.15)	-	2.68 (0.11)	-
18.8	53 (17)	-	-	-	0.89 (0.27)	-	3.84 (0.16)	-
20.0	55 (12)	1.25 (0.23)	182 (14)	28 (1)	1.00 (0.04)	0.033 (0.004)	4.9 (0.2)	0.12 (0.03)
21.0	62 (8)	-	197 (94)	-	1.01 (0.04)	-	4.8 (0.1)	-
23.6	69 (0)	2.53 (0.02)	174 (19)	31 (3)	1.91 (0)	0.07 (0.01)	4.1 (0.1)	0.16 (0.01)
29.1	74 (1)	1.30 (0.70)	132(25)	24 (1)	1.42 (0.25)	0.052 (0.001)	3.4 (1)	0.14 (0)
38.4	77 (2)	1.47 (0.81)	175 (10)	27 (2)	1.54 (0.09)	0.033 (0.001)	3.88 (0.04)	0.20 (0.01)
39.0	76 (8)	-	87 (6)	-	1.64 (0.09)	-	3.9 (0.4)	-
39.9	66 (0)	-	160 (21)	-	1.04 (0.05)	-	3.95 (0.40)	-
45.3	113 (12)	-	-	-	2.56 (0.05)	-	5.95 (0.35)	-
46.2	126 (2)	0.71 (0.24)	151 (14)	23 (1)	2.02 (0.21)	0.021 (0.001)	6.13 (0.54)	0.079 (0.001)
61.4	86 (0)	-	135 (9)	-	1.32 (0.03)	-	7.6 (0.2)	-

C_{SF} wt%	Code	E / MPa		σ_f / MPa		σ_{comp} / MPa		$\sigma_{plateau}$ / MPa	
		dry	swollen	dry	swollen	dry	swollen	dry	swollen
4.2	SN-4	7 (2)	0.034 (0.004)	16 (2)	9.3 (0.1)	0.13 (0.02)	0.008 (0.0001)	0.32 (0.01)	0.0085 (0)
13.4	DN-4/7	11.2 (0.1)	0.42 (0.09)	28 (5)	19 (2)	0.24 (0.05)	0.021 (0.004)	1.7 (0.1)	0.048 (0.002)
21	DN-4/14	35 (3)	1.2 (0.3)	43 (4)	23 (3)	0.77 (0.13)	0.034 (0.008)	3.0 (0.3)	0.13 (0.01)
28	DN-4/21	68 (11)	1.4 (0.3)	205 (24)	32 (2)	1.6 (0.7)	0.040 (0.009)	4.2 (1.2)	0.15 (0.03)
36	DN-4/29	58 (15)	1.6 (0.6)	240 (24)	24 (4)	2.8 (0.8)	0.037 (0.015)	4.7 (0.5)	0.22 (0.03)
45.4	TN-4/7/20	48 (11)	0.8 (0.1)	190 (12)	18 (3)	1.5 (0.6)	0.023 (0.002)	3.4 (0.5)	0.09 (0.01)

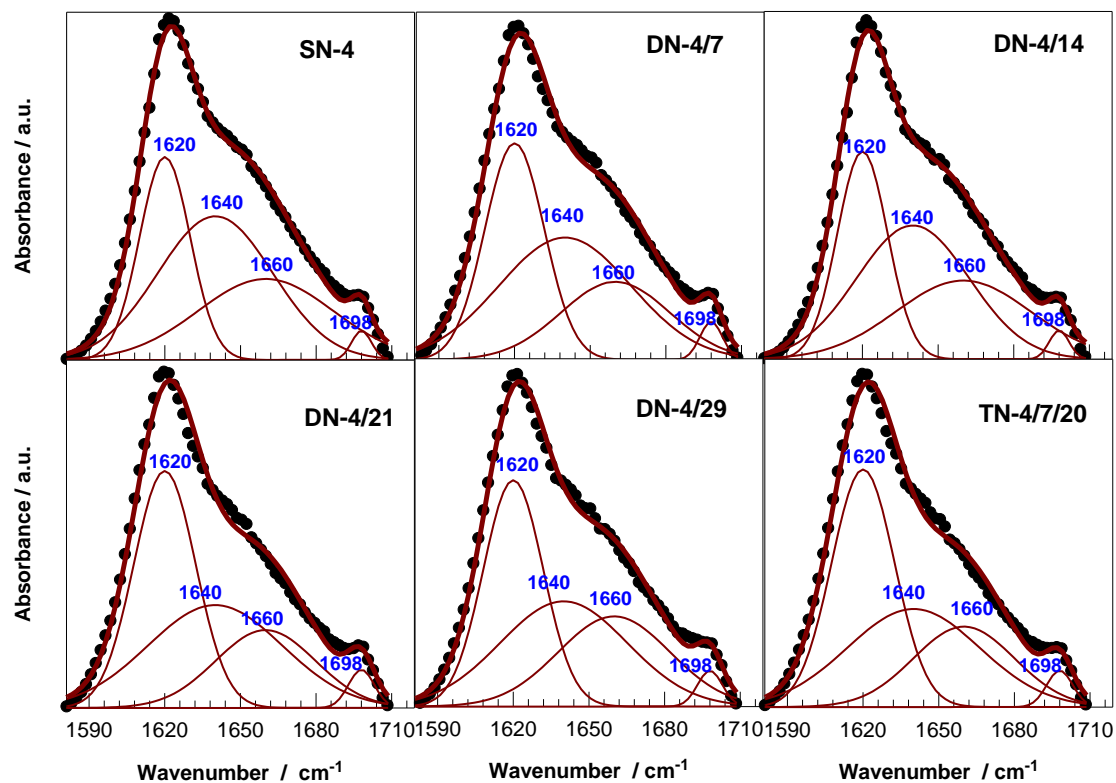


Figure S1. Typical ATR-FTIR spectra of SN, DN, and TN fibroin scaffolds after baseline correction. Amide I band regions of the spectra presenting the carbonyl stretching vibration of amide groups on silk fibroin are shown. The original data are shown by the filled circles while solid curves are the results of curve fitting for the original spectrum (thick curve) and hidden peaks (thin curves). All scaffolds display a main peak at 1620 cm^{-1} assigned to β -sheet conformation. In addition to the main peak, shoulders at 1660 and 1698 cm^{-1} are seen in the figures, which are assigned to α -helix and β -turn conformations, respectively. To estimate fibroin conformation, peak separation of Amide I band was carried out by selecting a Gaussian model for curve fitting, as described previously (refs. [18,48] in the text). The peak positions were fixed at 1620 , 1640 , 1660 , and 1698 cm^{-1} , representing β -sheet, random coil, α -helix, and β -turn conformations, respectively.

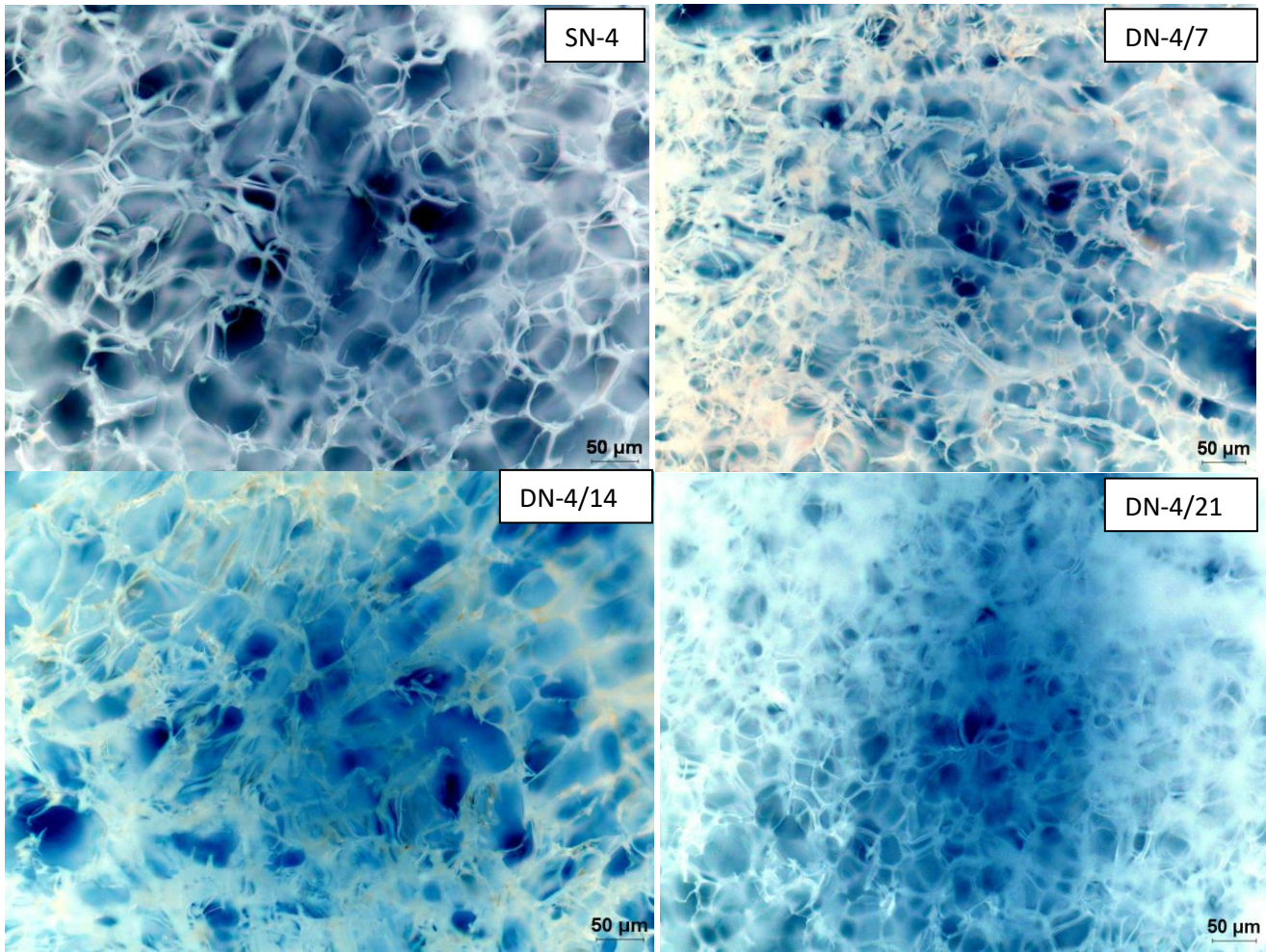


Figure S2. Optical microscopy images of SN and DN cryogels. Scaling bars are 50 μm .

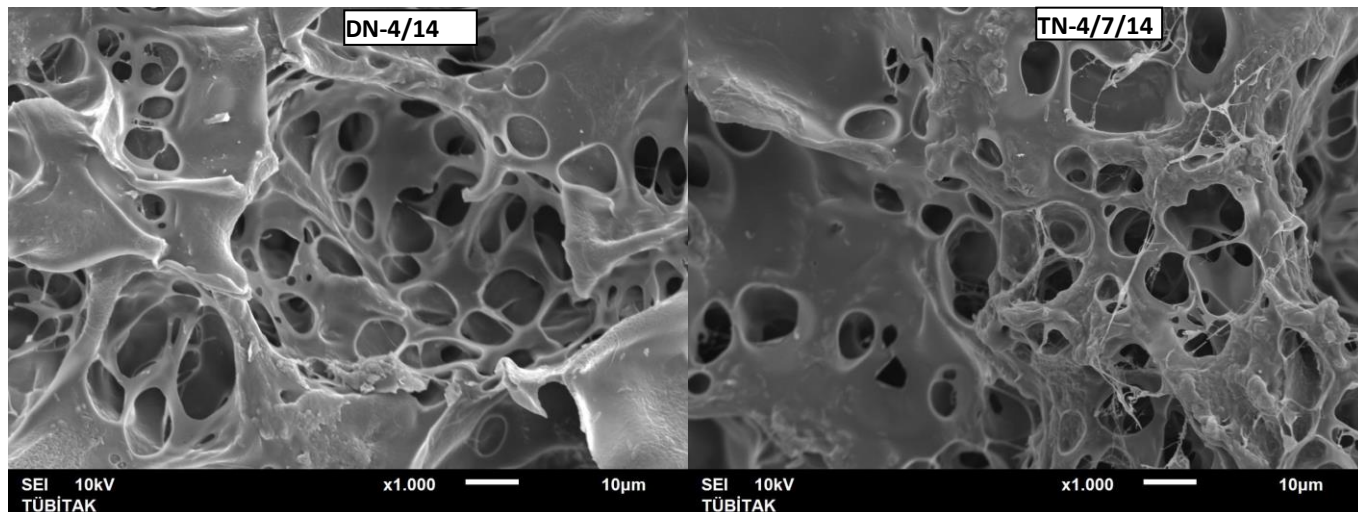


Figure S3. SEM images of DN-4/14 and TN-4/4/14 fibroin scaffolds. Scaling bars = 10 μm
(Magnification = x1000).